

SUPPLEMENTARY INFORMATION

Selective Optical Assembly of Highly Uniform Nanoparticles by Doughnut-Shaped Beams

Syoji Ito^{1,2,3*}, Hiroaki Yamauchi^{1,2}, Mamoru Tamura^{4,5}, Shimpei Hidaka^{4,5}, Hironori Hattori^{4,5}, Taichi Hamada^{4,5}, Keisuke Nishida^{4,5}, Shiho Tokonami⁴, Tamitake Itoh⁶, Hiroshi Miyasaka^{1,2}, and Takuya Iida^{3,4*}

¹Division of Frontier Materials Science, Graduate School of Engineering Science, Osaka University, Toyonaka, Osaka 560-8531, Japan

²Center for Quantum Materials Science under Extreme Conditions, Osaka University, Toyonaka, Osaka 560-8531, Japan

³PRESTO, Japan Science and Technology Agency, 4-1-8 Honcho, Kawaguchi, Saitama 332-0012, Japan

⁴Nanoscience and Nanotechnology Research Center, Osaka Prefecture University, 1-2, Gakuencho, Nakaku, Sakai, Osaka 599-8570, Japan

⁵Graduate School of Engineering, Osaka Prefecture University, 1-1, Gakuen-cho, Nakaku, Sakai, Osaka 599-8531, Japan

⁶Health Research Institute, National Institute of Advanced Industrial Science and Technology (AIST), Takamatsu, Kagawa 761-0395, Japan

Correspondence and requests for materials should be addressed

to T. Iida (t-iida@21c.osakafu-u.ac.jp) and S. Ito (sito@chem.es.osaka-u.ac.jp).

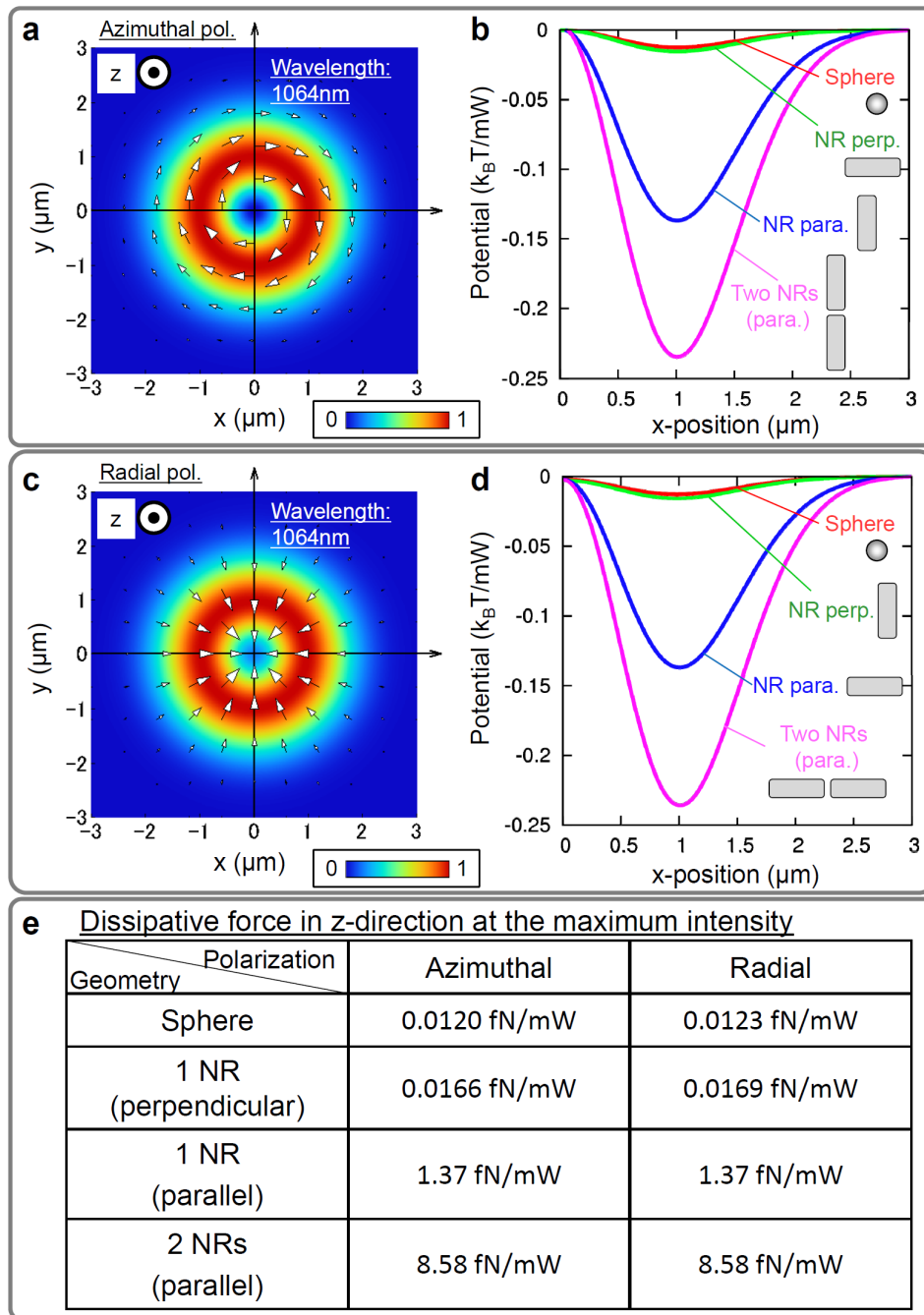
Supplementary Movies

Supplementary Movie S1 | Assembling process of silver nanorods by a radially polarized beam. A ring-like assembled structure of silver nanorods (AgNRs) is growing at the left bottom under the irradiation of radially-polarized beam of 23.8 mW power at the sample (120 mW just after the radial converter) with the same intensity distribution as that in the inset of Fig. 2c. During the concentric ring pattern with bright spot (laser of 488 nm wavelength as a monitor) appears or disappears at upper right, the doughnut beam of 1064 nm wavelength is turned off and on, respectively. The length of each side in the movie is 16.7 μm , and was recorded with 7.33 frames/s (136 ms per 1 frame) 32.5 nm/pixel in the original file.

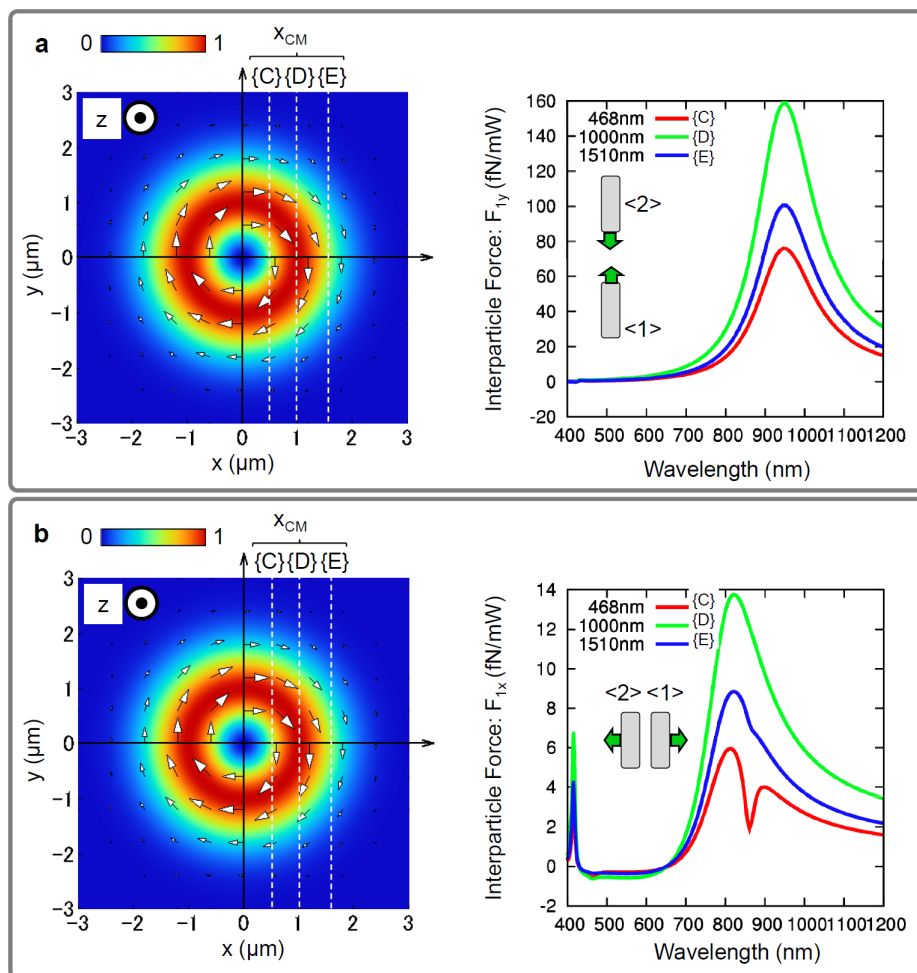
Supplementary Movie S2 | Simulated assembling process of silver nanorods by azimuthally polarized beam. The Monte Carlo simulation was performed to investigate the behavior of Ag NRs under the self-consistently evaluated light-induced force of doughnut beam based on the Equations (1)-(3) in **Methods** of the main text. In the initial configuration, 36 Ag NRs are arranged in square lattice with random orientations, where the centre of mass coordinates of neighbor Ag NRs are separated with 500 nm. In each Monte Carlo step, each Ag NR randomly experiences 1 nm parallel displacement and 1° rotation (3 types rotations are considered around the center of mass of Ag NR, the end of Ag NR, and the other end of Ag NR). The configuration of Ag NRs was recorded every 50 steps. We can see the tendency that Ag NRs are fluctuated but oriented parallel to the polarizations at high intensity positions of the doughnut beam. Parameters of DLVO potential in water are given in reference to Ref. 15. Spot diameter is 2 μm , laser Power is 25 mW, the number of total steps is 100,000, and the environmental temperature is 298K.

Supplementary Movie S3 | Simulated assembling process of silver nanorods by radially polarized beam. Under the same conditions as Supplementary Movie S2 except for the polarization.

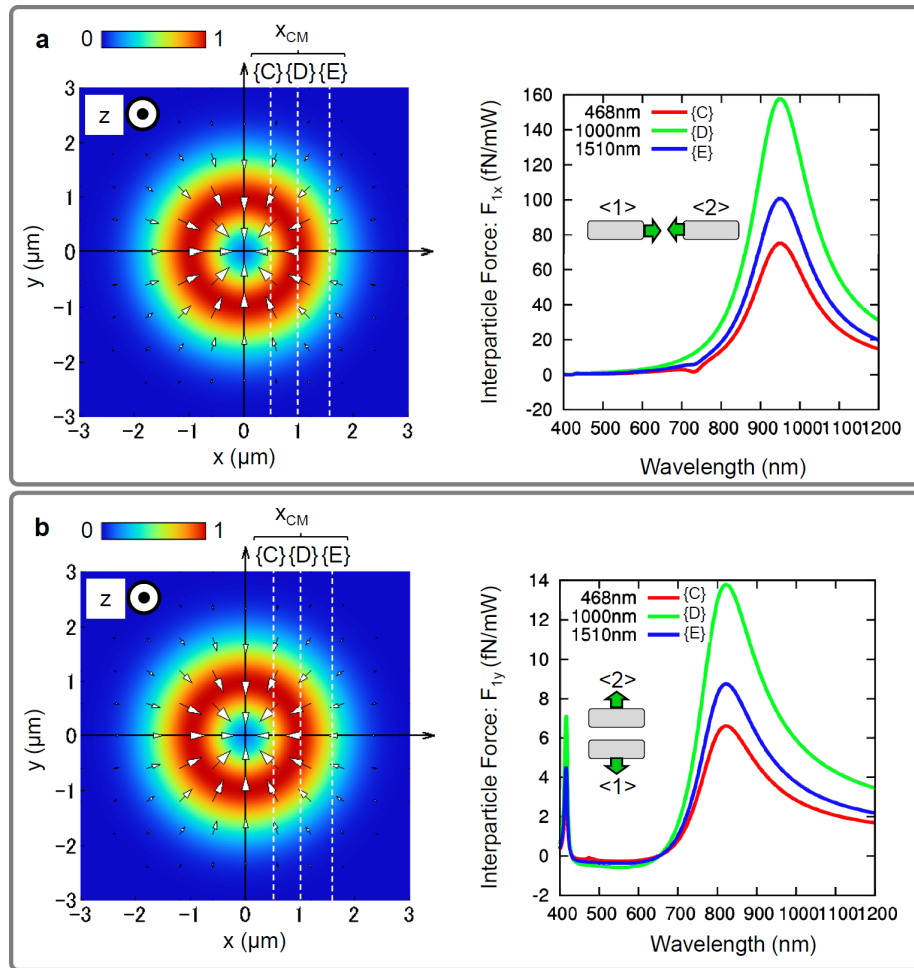
Supplementary Figures



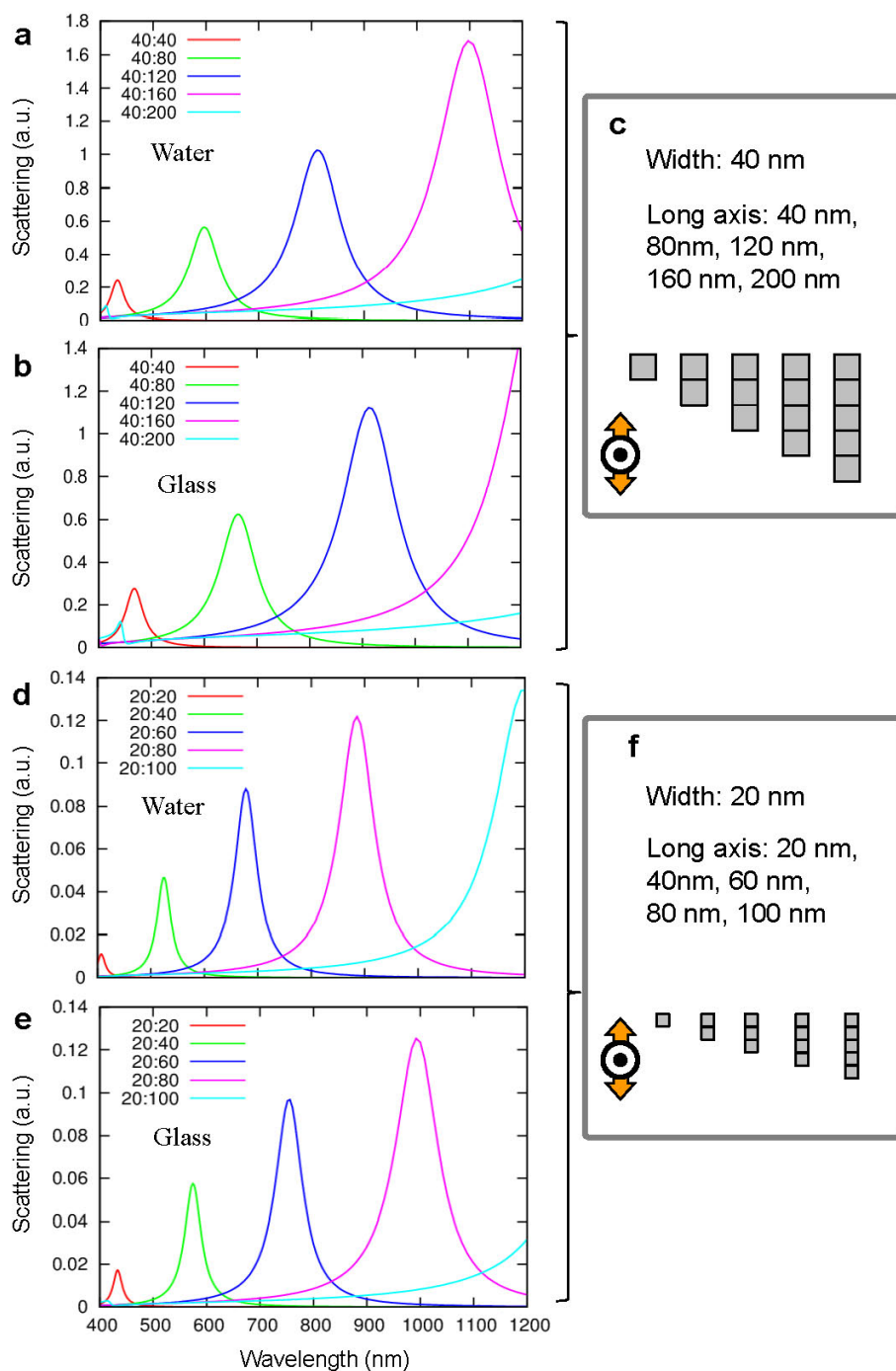
Supplementary Figure S1 | Numerical evaluation of the optical potential and dissipative force exerted on Ag nanorods for different polarizations. **a**, Spatial distribution of the electric field intensity (normalized by the maximum intensity) and polarization vectors of the azimuthally polarized beam. **b**, Position dependence of the optical potential well along the x -axis for a spherical Ag NP (60 nm in diameter); a single Ag NR (40 x 120 nm) aligned parallel or perpendicular to the azimuthal polarization; and two Ag NRs of separation 30 nm, aligned parallel to the polarization. **c**, **d** As for **a** and **b** for the radially polarized beam. **e** Summary of the dissipative force along the beam propagation direction for the different configurations (the centre of mass of the pair of NRs was taken as the position (1000 nm, 0 nm, 0 nm)). Throughout **a-e**, the wavelength was chosen to be 1064 nm - corresponding to the value used in the experiment.



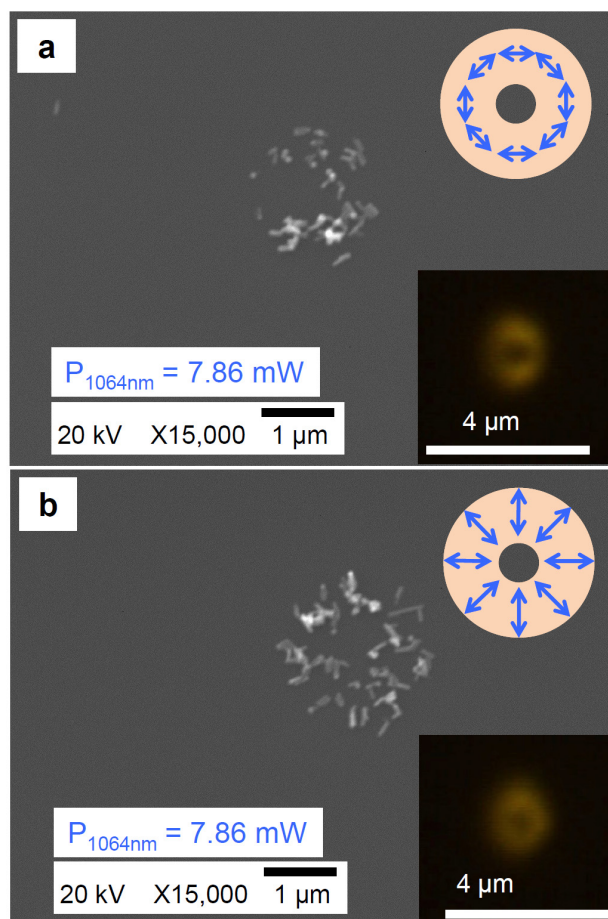
Supplementary Figure S2 | Calculated spectra of interparticle light-induced force between two Ag NRs (40 nm wide, 120 nm long, 30 nm separation) for azimuthal polarization. **a** and **b**, x - and y -components of the force on NR <1> in the geometries of respective left figures indicating azimuthally and radially polarized beams, where an opposite force is exerted on NR <2>. The coordinate of the centre of mass of the NRs (X_{CM} , $Y_{CM}=0$, $Z_{CM}=0$) was set to three different positions: {C} ($X_{CM}=468$ nm) indicates the position with the steepest intensity gradient inside of the doughnut; {D} ($X_{CM}=1000$ nm) indicates the position with the highest intensity; and {E} ($X_{CM}=1510$ nm) indicates the position with the steepest intensity gradient outside of the doughnut. In **a**, two Ag NRs are arranged to be coaxial and parallel to the polarization at the same radial coordinate and a different azimuth angle. Due to the coaxial induced polarization with the same direction in the NRs, a strong attractive force arises between the NRs via the longitudinal wave. In **b**, two Ag NRs are arranged head-to-head and parallel to the polarization, with the same azimuth angle. In this case, a weaker repulsive force arises between the NRs via the transverse wave.



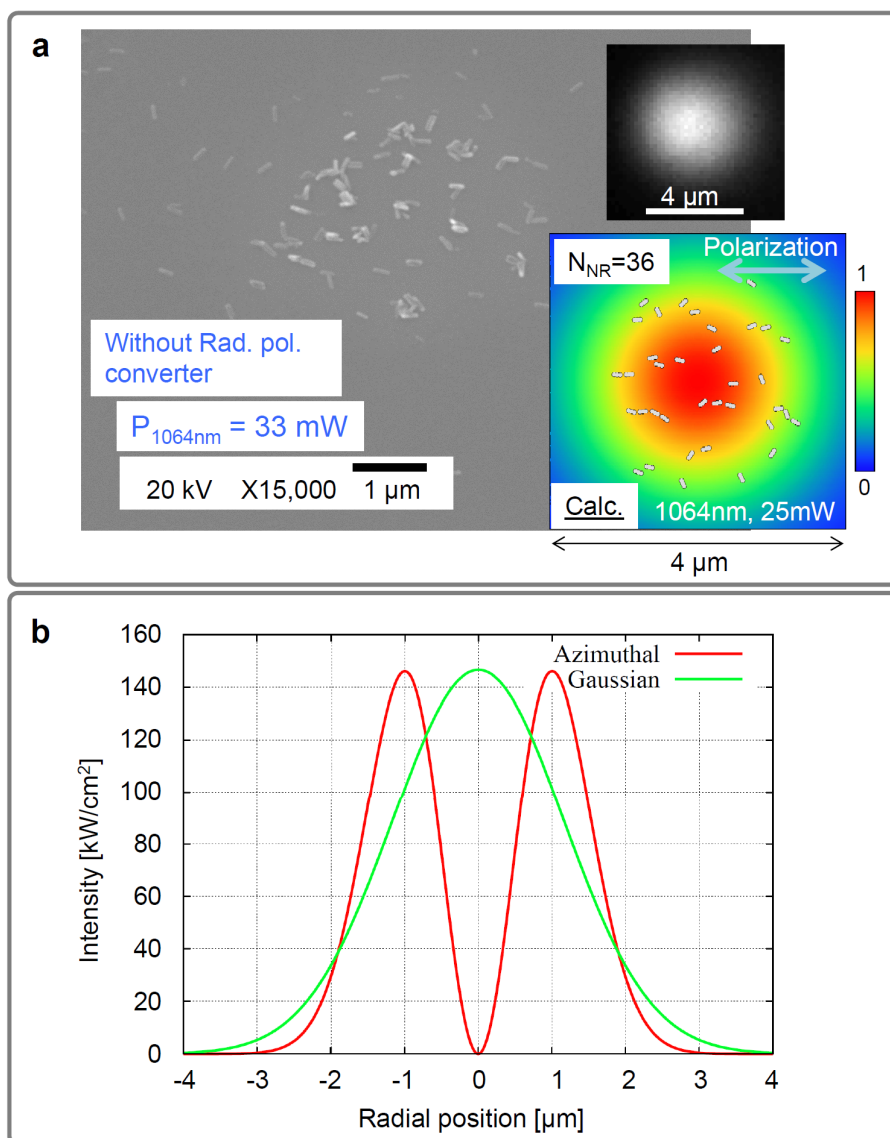
Supplementary Figure S3 | Calculated spectra of interparticle light-induced force between two Ag NRs (40 nm wide, 120 nm long, 30 nm separation), for radial polarization. a and b, x - and y -components of the force on NR <1> in the geometries of respective left figures indicating azimuthally and radially polarized beams, where an opposite force is exerted on NR <2>. The coordinate of centre of mass of the NRs (X_{CM} , $Y_{CM}=0$, $Z_{CM}=0$) was set to three different positions: {C} ($X_{CM}=468$ nm) indicates the position with the steepest intensity gradient inside of the doughnut; {D} ($X_{CM}=1000$ nm) indicates the position with the highest intensity; and {E} ($X_{CM}=1510$ nm) indicates the position with the steepest intensity gradient outside of the doughnut. In **a, two Ag NRs are arranged to be coaxial and parallel to the polarization at the same radial coordinate and a different azimuth angle. Due to the coaxial induced polarization with the same direction in the NRs, a strong attractive force arises between the NRs via the longitudinal wave. In **b**, two Ag NRs are arranged head-to-head and parallel to the polarization, with the same azimuth angle. In this case, a weaker repulsive force arises between the NRs via the transverse wave.**



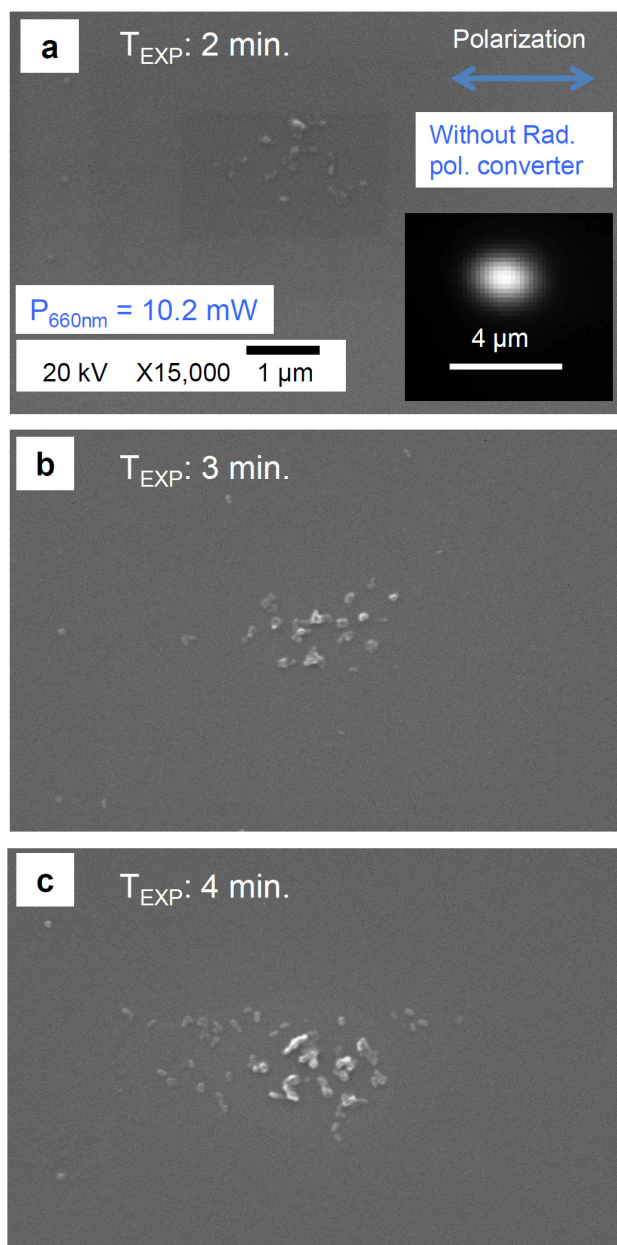
Supplementary Figure S4 | Calculated scattering spectra from single Ag NRs with different aspect ratio for two types of widths. a and b, Width of 40 nm and an aspect ratio ranging from 1 to 5 as shown in **c** with water (refractive index=1.33) and glass (refractive index=1.51) as surrounding mediums, respectively. **d and e,** Scattering spectra of NRs with a width of 20 nm and an aspect ratio ranging from 1 to 5 in water and glass as shown in **f**. Although a small number of cubic discretized cells and parallel polarization were assumed, as shown in the schematic illustrations in **c** and **f**, to solve the integral of Maxwell equations, it was confirmed that our results correctly reproduced the results of Whiley *et al.*²⁵, where the synthesis of Ag NRs by a different chemical method was reported



Supplementary Figure S5 | Electron microscope images of the Ag nanorods selected by doughnut laser beams with small beam spot diameter. (a) Scanning electron microscope (SEM) image of Ag NRs selected by the azimuthally polarized doughnut beam. **(b)** Scanning electron microscope (SEM) image of Ag NRs selected by the radially polarized doughnut beam. In both cases of (a) and (b), doughnut beams with small diameter in comparison with the case in Fig. 2 were used for optical assembling. The insets of **(a)** and **(b)** show the schematic of the respective polarization (upper), and the intensity distribution of the doughnut beam as visualized by two photon imaging (lower).



Supplementary Figure S6 | Electron microscope images of the Ag nanorods selected by Gaussian laser beams with 1064 nm wavelength. (a) SEM image of Ag NRs selected by linearly-polarized Gaussian beam. The insets show the intensity distribution of the Gaussian beam as visualized by two photon imaging (upper), and a simulation result of Ag NRs under the irradiation of linearly-polarized Gaussian beam with conditions similar to the experiment (lower). **(b)** Spatial profiles in the radial direction of azimuthally-polarized doughnut beam and Gaussian beam with the same maximum intensity and input power.



Supplementary Figure S7 | Electron microscope images of the Ag nanoparticles selected by Gaussian laser beams with 660 nm wavelength and small spot diameter. (a)-(c) SEM images of Ag NPs with low aspect ratio selected by linearly-polarized Gaussian beam with small spot diameter for different irradiation times (T_{EXP}). The inset in (a) shows the intensity distribution of the Gaussian beam through (a)-(c) as visualized by one photon imaging.